

*Experimental search for collapse signal at Gran Sasso*  
*K. Piscicchia\**

*Mini-symposium Quantum Boundaries: Gravity Related Collapse  
Models*  
*22 December 2021*

*\*Centro Ricerche Enrico Fermi, LNF (INFN)*  
*kristian.piscicchia@cref.it*

## Contents:

- *Brief introduction to the Collapse Models*
- *Lower bound on the  $R_0$  parameter of the gravity-related Diòsi-Penrose (DP) model.*
- *Constraint on the  $\Lambda/r_c^2$  parameter of the Continuous Spontaneous Localization model.*
- *Ongoing and future experimental activity*

# *Dynamical reduction models, a brief introduction*

*Why the quantum properties of microscopic systems, most notably, the possibility of being in the superposition of different states at once, do not seem to carry over to larger objects? A debate which is as old as the quantum theory itself.*

*Even perfectly isolating a quantum system, regardless its size, will the linear and deterministic shroedinger evolution manifest forever? -> direct impact on Quantum Technologies*

*Superposition principle may progressively break down when atoms glue together to form larger systems*

*[Károlyhazi, Diósi, Lukács, Penrose, Ghirardi, Rimini, Weber, Pearle, Adler, Milburn, Bassi ...]*

*But what triggers the w.f. Collapse?*

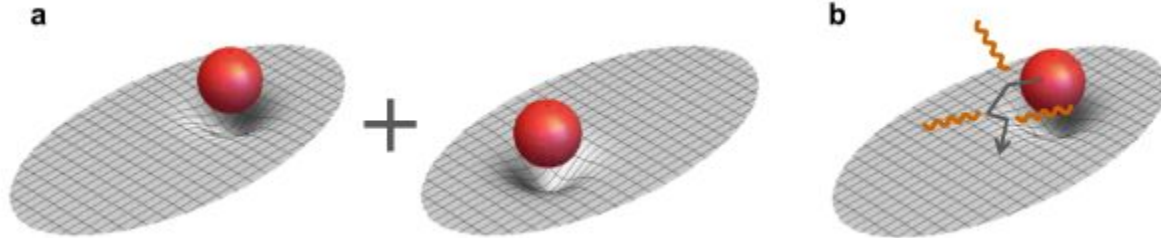
*Feynman in lectures on gravitation: breakdown of the quantum superposition at macroscopic scale, possibility that gravity might not be quantized.*

# Gravity induced collapse

*Diósi: QT requires an absolute indeterminacy of the gravitational field, -> the local gravitational potential should be regarded as a stochastic variable, whose mean value coincides with the Newton potential, and the correlation function is:*

$$\langle \phi(\mathbf{r}, t) \phi(\mathbf{r}', t') \rangle - \langle \phi(\mathbf{r}, t) \rangle \langle \phi(\mathbf{r}', t') \rangle \sim \frac{\hbar G}{|\mathbf{r} - \mathbf{r}'|} \delta(t - t')$$

*Penrose: When a system is in a spatial quantum superposition, a corresponding superposition of two different space-times is generated. The superposition is unstable and decays in time. The more massive the system in the superposition, the larger the difference in the two space-times and the faster the wave-function collapse.*



# Gravity induced collapse

$$d|\psi_t\rangle = \left[ \underbrace{-\frac{i}{\hbar} \hat{H} dt}_{\text{Schrödinger}} + \underbrace{\sqrt{\frac{G}{\hbar}} \int d\mathbf{x} (\hat{\mu}(\mathbf{x}) - \langle \hat{\mu}(\mathbf{x}) \rangle) dW_t(\mathbf{x}) - \frac{G}{2\hbar} \int d\mathbf{x} d\mathbf{y} \frac{(\hat{\mu}(\mathbf{x}) - \langle \hat{\mu}(\mathbf{x}) \rangle) (\hat{\mu}(\mathbf{y}) - \langle \hat{\mu}(\mathbf{y}) \rangle)}{|\mathbf{x} - \mathbf{y}|} dt}_{\text{Collapse}} \right] |\psi_t\rangle$$

- Collapse in position;
- Amplification mechanism.

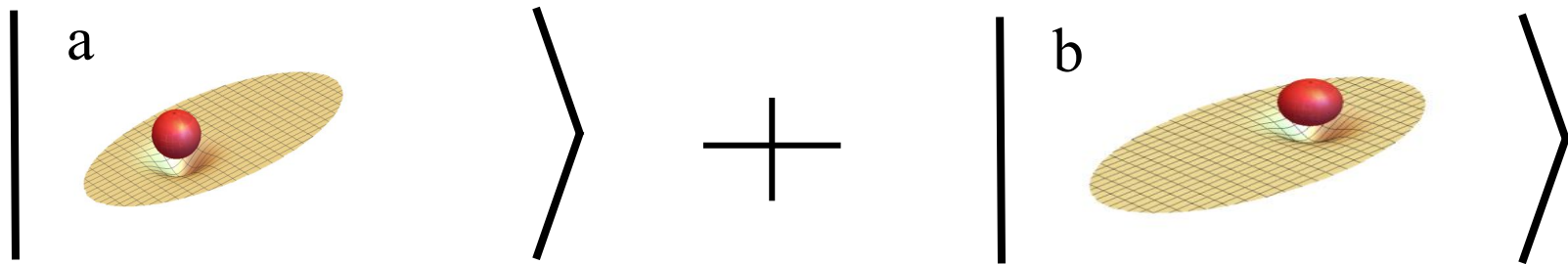
 Schrödinger  
 Collapse

$$\frac{d\hat{\rho}(t)}{dt} = -\frac{i}{\hbar} [\hat{H}, \hat{\rho}(t)] - \frac{G}{2\hbar} \int \frac{d\mathbf{x} d\mathbf{y}}{|\mathbf{x} - \mathbf{y}|} [\hat{\mu}(\mathbf{x}), [\hat{\mu}(\mathbf{y}), \hat{\rho}(t)]]$$

$$\rho(\mathbf{a}, \mathbf{b}, t) = \rho(\mathbf{a}, \mathbf{b}, 0) e^{-t/\tau}$$

$$\tau^{-1} = \frac{G}{2\hbar} \int d\mathbf{x} d\mathbf{y} \frac{(\hat{\mu}_a(\mathbf{x}) - \hat{\mu}_b(\mathbf{x})) (\hat{\mu}_a(\mathbf{y}) - \hat{\mu}_b(\mathbf{y}))}{|\mathbf{x} - \mathbf{y}|}$$

# Gravity induced collapse



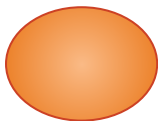
$$\Delta E_{\text{DP}} = 4\pi G \int d\mathbf{r} \int d\mathbf{r}' \frac{[\mu_a(\mathbf{r}) - \mu_b(\mathbf{r})] [\mu_a(\mathbf{r}') - \mu_b(\mathbf{r}')] }{|\mathbf{r} - \mathbf{r}'|}.$$

$$\tau_{\text{DP}} = \frac{\hbar}{\Delta E_{\text{DP}}}$$



Proton:  $m \approx 10^{-27}$  Kg,  $R \approx 10^{-15}$  m

$\tau_{\text{DP}} \approx 10^6$  years



Dust grain:  $m \approx 10^{-12}$  Kg,  $R \approx 10^{-5}$  m

$\tau_{\text{DP}} \approx 10^{-8}$  s

# Gravity induced collapse

The DP theory is parameter-free, but the gravitational self energy difference diverges for point-like particles  $\rightarrow$  a short-length cutoff  $R_0$  is introduced to regularize the theory.

Diósi: minimum length  $R_0$  limits the spatial resolution of the mass density, a short-length cutoff to regularize the mass density. EG becomes a function of  $R_0$  the larger  $R_0$  the longer the collapse time.

Penrose: Penrose - which are the basic stable states to which the superposition decays? They are the stationary solutions of the Shroedinger-Newton equation.  $R_0$  is the size of the particle mass density.

$$\mu(\mathbf{r}) = m|\psi(\mathbf{r}, t)|^2$$

# Gravity induced collapse, direct test

*Direct tests: creating a large superposition of a massive system, to guarantee that decay time is short enough for the collapse to become effective before any kind of external noise disrupts the measurement, matter-wave interferometry with macromolecules, phononic states, experiments in space: no gravity ---> more time (MAQRO, CAL, etc..).*

*Kovachy, T. et al. Quantum superposition at the half-metre scale. Nature 528, 530–533 (2015).*

*Fein, Y. Y. et al. Quantum superposition of molecules beyond 25 kDa. Nature Physics 15, 1242–1245 (2019).*

*Lee, K. C. et al. Entangling macroscopic diamonds at room temperature. Science 334, 1253–1256 (2011).*

# Testing collapse models by means of Gamma ray spectroscopy

Indirect tests of collapse models exploit an unavoidable side effect of the collapse: a Brownian-like diffusion of the system in space.

Collapse probability is Poissonian in  $t$  -> Lindblad dynamics for the statistical operator -> free particle average square momentum increases in time.

Then charged particles emit *spontaneous radiation*. We search for spontaneous radiation emission from a germanium crystal and the surrounding materials in the experimental apparatus.

Strategy: simulate the background from all the known emission processes -> perform a Bayesian comparison of the residual spectrum with the theoretical prediction -> extract the pdf of the model parameters -> bound the parameters.

# The LNGS laboratories environment

*The experiment was carried out in the low-background environment of the underground Gran Sasso National Laboratory of INFN:*

- *overburden corresponding to a minimum thickness of 3100 m w.e.*
- *cosmic radiation flux is reduced by almost six orders of magnitude, to a flux of three  $\mu\text{m}^2$ .*
- *the main background source consists of  $\gamma$ -radiation produced by long-lived  $\gamma$ -emitting primordial isotopes and their decay products.*



# Theoretical prediction for the expected spontaneous emission rate

- *CSL - s. e. photons rate:*

$$\frac{d\Gamma_t}{d\omega} = \frac{\lambda \hbar e^2 N^2 N_a}{4\pi^2 \epsilon_0 c^3 m_0^2 r_C^2 E}$$

- *DP - s. e. photons rate:*



*Calculated in collaboration with L. Diosi, A. Bassi & S. Donadi*

*In our range  $\Delta E = (1 - 4)$  MeV electrons are relativistic, only the contribution of protons ( $N$ ) is considered.*

$\Lambda$  - collapse strength

$r_c$  - correlation length

see e. g. S. L. Adler, *JPA* 40, (2007) 2935, Adler, S.L.; Bassi, A.; Donadi, S., *JPA* 46, (2013) 245304.

$R_0$  - size of the particle mass density. See e.g. Diósi, L. *J. Phys. Conf. Ser.* 442, 012001 (2013)., Penrose, R. *Found. Phys.* 44, 557–575 (2014).

# The experimental setup

The experimental apparatus is based on a coaxial p-type high purity germanium detector (HPGe):

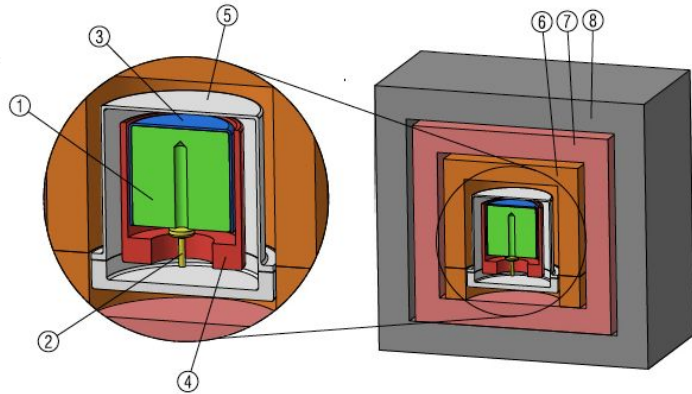
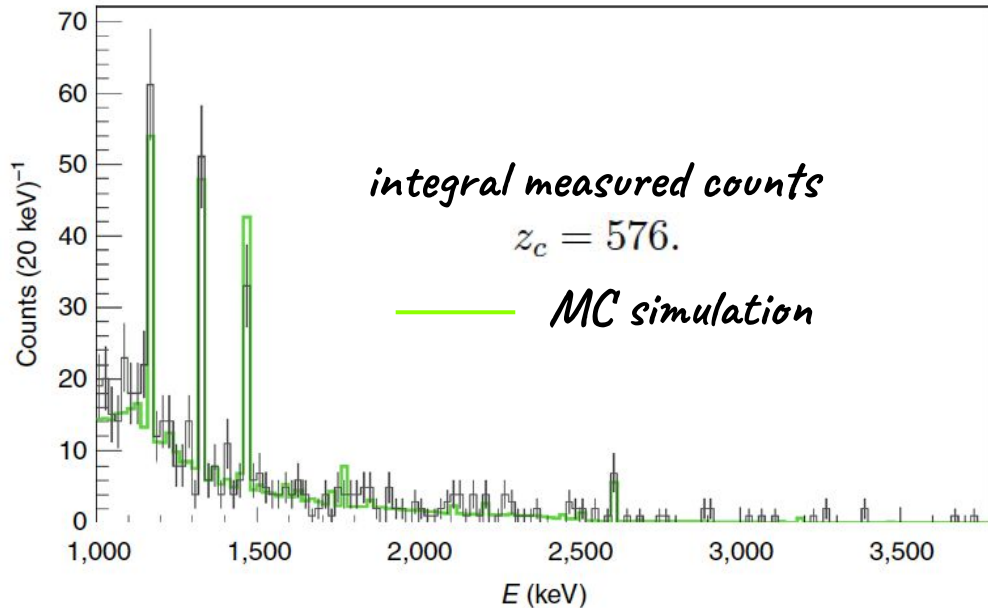


Figure 1: Schematic representation of the experimental setup: 1 - Ge crystal, 2 - Electric contact, 3 - Plastic insulator, 4 - Copper cup, 5 - Copper end-cup, 6 - Copper block and plate, 7 - Inner Copper shield, 8 - Lead shield.

- Exposure  $124 \text{ kg} \cdot \text{day}$ ,  $m_{\text{Ge}} \sim 2 \text{ kg}$
- on the bottom and on the sides 5 cm thick borated polyethylene plates give a partial reduction of the neutron flux
- an airtight steel housing encloses the shield and the cryostat, flushed with boil-off nitrogen to minimize the presence of radon.

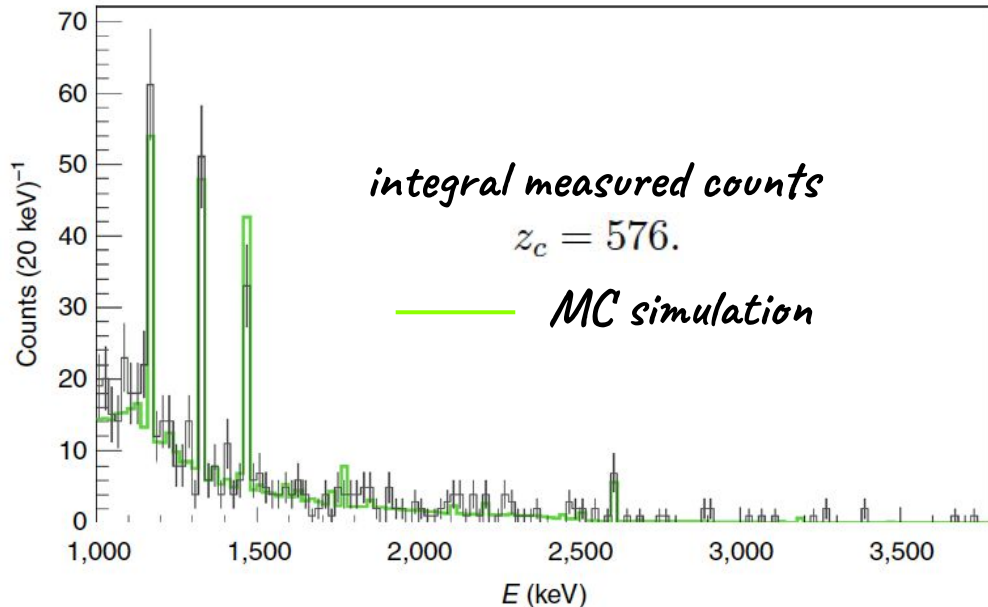
# Measured spectrum and background simulation

The spectrum only contains “real events” as the digital DAQ system has a filter rejecting noise events, by their pulse shape, with efficiency better than 99%.



# Measured spectrum and background simulation

The experimental apparatus is characterised, through a validated MC code, based on the GEANT-4 software library. The background is due to emission of residual radio-nuclides:



- the activities are measured for each component
- the MC simulation accounts for:
  1. emission probabilities and decay schemes for each radio-nuclide in each material
  2. photons propagation and interactions
  3. detection efficiencies.

The simulation describes 88% of the integral counts:

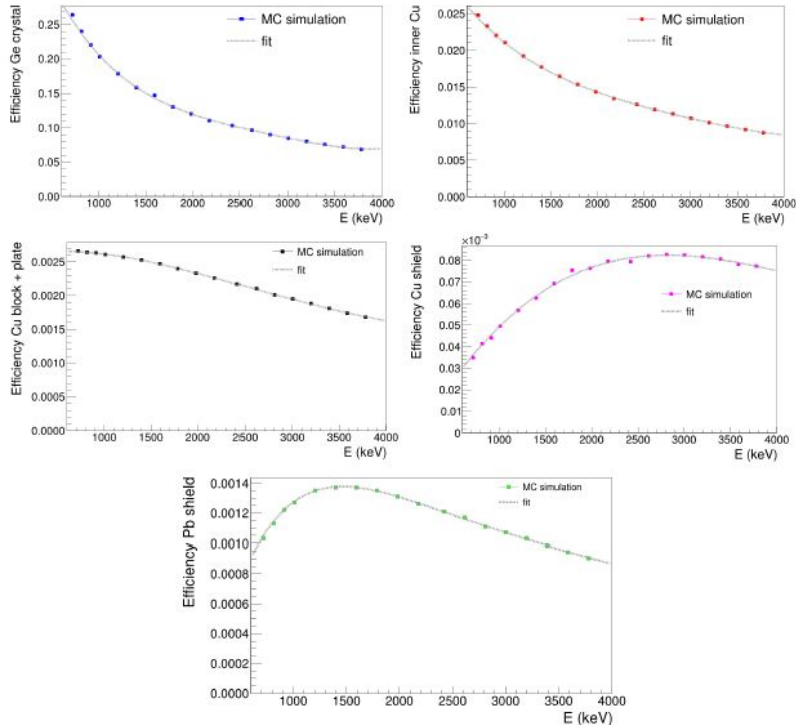
$$z_{b,ij} = \frac{m_i A_{ij} T N_{rec,ij}}{N_{ij}}, \quad z_b = \sum_{i,j} z_{b,ij} = 506.$$

*Gravity-related wave function collapse models ..*

*lower bound on  $R_0$*

# Lower bound on $R_0$ expected signal contribution

The expected number of photons spontaneously emitted by the nuclei of all the materials of the detector are obtained weighting the theoretical rate for the detection efficiencies:



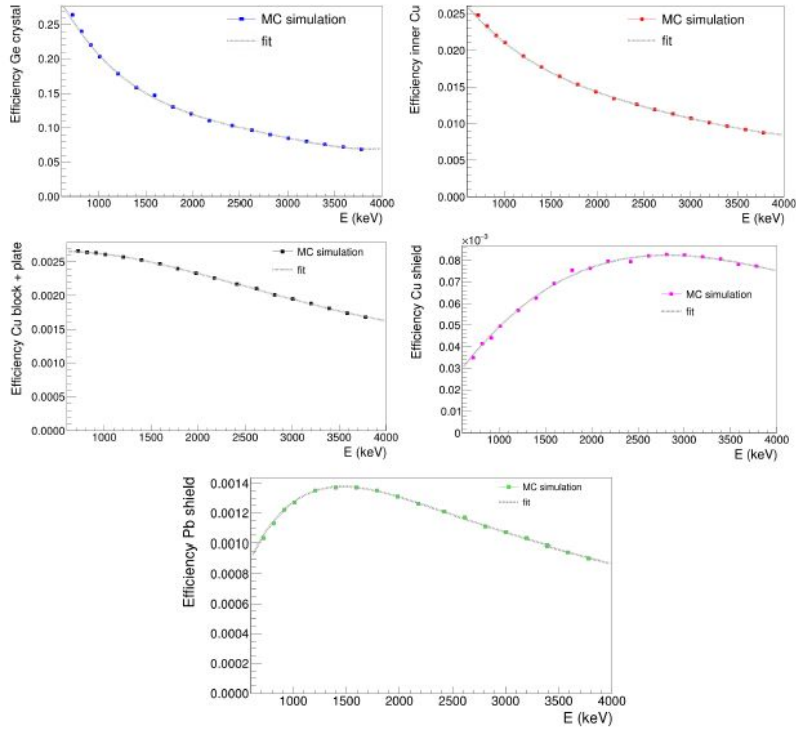
- $10^8$  photons generated for each energy for each material
- efficiency functions are obtained by polinomial fits  $\epsilon_i(E) = \sum_{j=0}^{c_i} \xi_{ij} E^j$
- the expected signal contribution is:

$$z_s(R_0) = \sum_i \int_{\Delta E} \frac{d\Gamma_t}{dE} \Big|_i T \epsilon_i(E) dE = \frac{a}{R_0^3}$$

with  $a = 1.8 \cdot 10^{-27} \text{ m}^3$

# Lower bound on $R_0$ expected signal contribution

The expected number of photons spontaneously emitted by the nuclei of all the materials of the detector are obtained weighting the theoretical rate for the detection efficiencies:



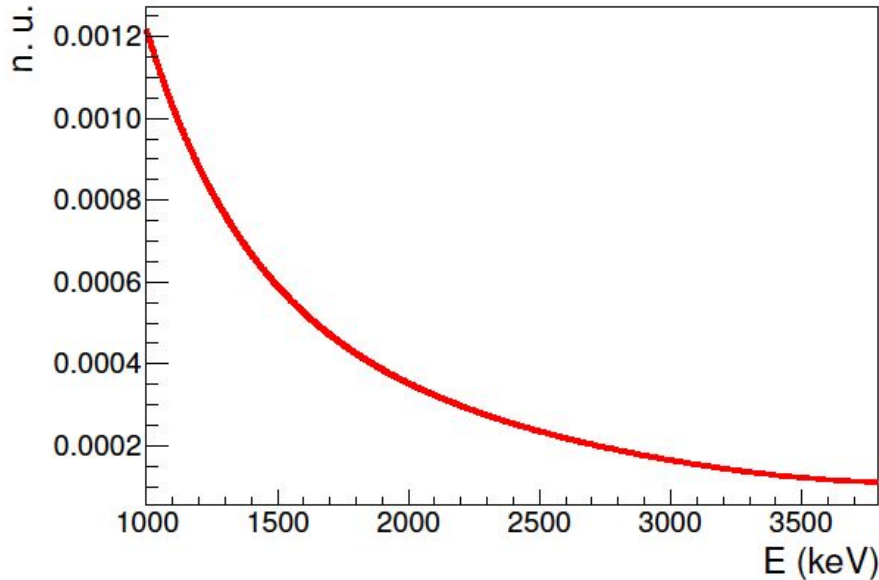
- $10^8$  photons generated for each energy for each material
- efficiency functions are obtained by polinomial fits  $\epsilon_i(E) = \sum_{j=0}^{c_i} \xi_{ij} E^j$
- the expected signal contribution is:

$$z_s(R_0) = \sum_i \int_{\Delta E} \frac{d\Gamma_t}{dE} \Big|_i T \epsilon_i(E) dE = \frac{a}{R_0^3}$$

with  $a = 1.8 \cdot 10^{-27} \text{ m}^3$

# Lower bound on $R_0$ expected signal contribution

The expected signal of spontaneously emitted photons by the nuclei of all the materials of the detector is obtained weighting the theoretical rate for the detection efficiencies:



Energy distribution of the expected signal,  
resulting from the sum of the emission rates of  
all the materials,  
weighted for the efficiency functions.  
The area of the distribution is normalised to the  
unity (n. u.)

# Lower bound on $R_0$

pdf of  $R_0$

$z_c$  is distributed according to a Poissonian  $p(z_c|\Lambda_c) = \frac{\Lambda_c^{z_c} e^{-\Lambda_c}}{z_c!}$  with  $\Lambda_c(R_0) = \Lambda_b + \Lambda_s(R_0)$

The pdf of  $R_0$  is then given by probability inversion:

$$\tilde{p}(\Lambda_c(R_0)|p(z_c|\Lambda_c(R_0))) = \frac{p(z_c|\Lambda_c(R_0)) \cdot \tilde{p}_0(\Lambda_c(R_0))}{\int_D p(z_c|\Lambda_c(R_0)) \cdot \tilde{p}_0(\Lambda_c(R_0)) d[\Lambda_c(R_0)]}$$

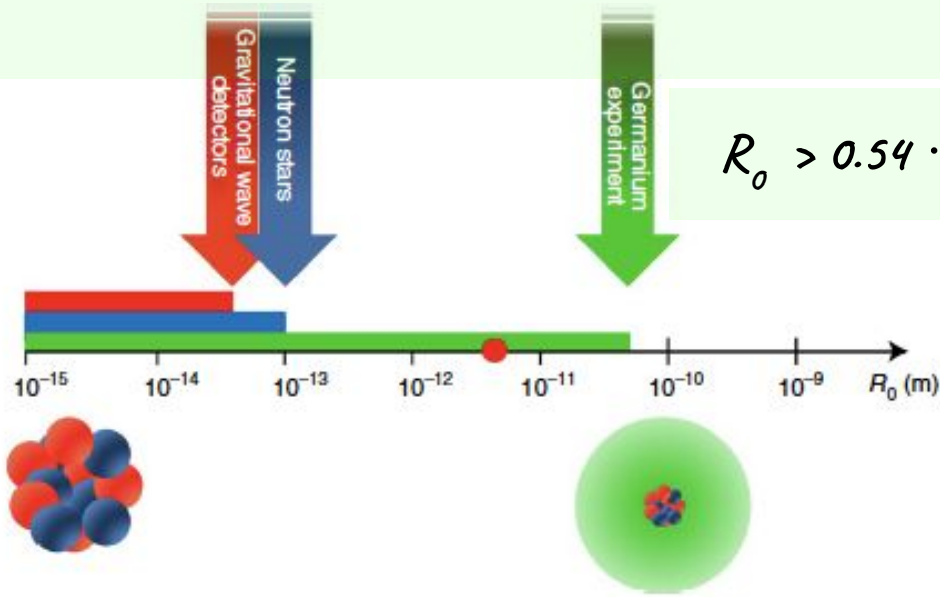
The prior  $\tilde{p}_0(\Lambda_c(R_0)) = \theta(\Lambda_c^{\max} - \Lambda_c(R_0))$  accounts for previous limits from gravitational wave detectors and neutron stars data analyses [Phys. Rev. D 95, 084054 (2017), Phys. Rev. Lett. 123, 080402 (2019)].

A bound on  $R_0$  is obtained from the cumulative pdf:

$$\tilde{P}(\bar{\Lambda}_c) = \frac{\gamma(z_c + 1, \bar{\Lambda}_c)}{\gamma(z_c + 1, \Lambda_c^{\max})} = 0.95$$

$$R_0 > 0.54 \cdot 10^{10} \text{ m}$$

# Lower bound on $R_0$



$$R_0 > 0.54 \cdot 10^{-10} \text{ m}$$

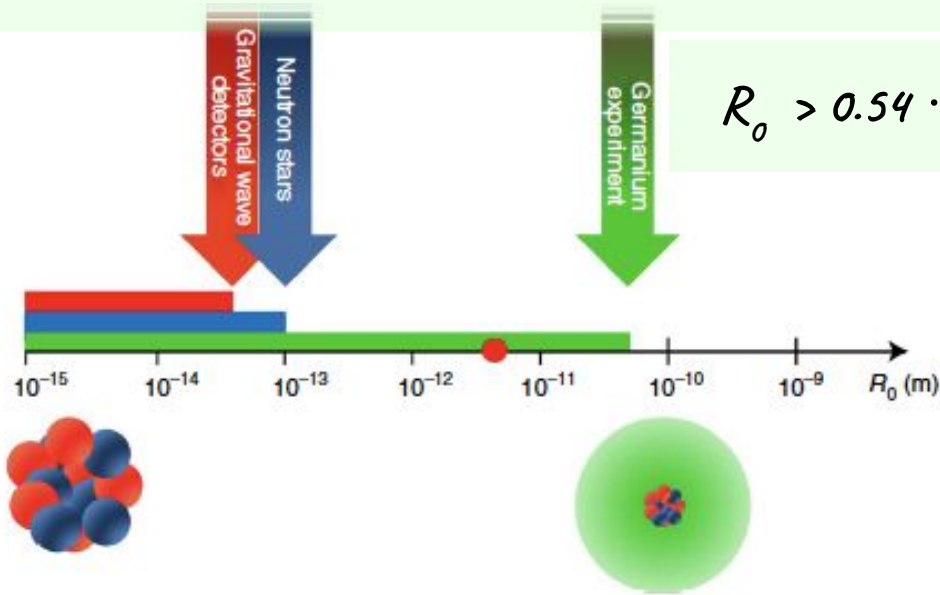
If  $R_0$  is the size of the nucleus's wave function as suggested by Penrose, we have to compare the limit with the properties of nuclei in matter.

In a crystal  $R_0^2 = \langle u^2 \rangle$  is the mean square displacement of a nucleus in the lattice, which, for the germanium crystal, cooled to liquid nitrogen temperature amounts to  $R_0 = 0.05 \cdot 10^{-10} \text{ m}$

*“Underground test of gravity-related wave function collapse”. Nature Physics 1–5, (2020).*

top 10 of all 2020 favorite scientific news stories <https://www.sciencemag.org/news/2020/12/our-favorite-science-news-stories-2020-non-covid-19-edition>

# Lower bound on $R_0$



$$R_0 > 0.54 \cdot 10^{10} \text{ m}$$

Penrose proposal is ruled out in present formulation!

Generalizations of the models are ongoing:

- add dissipation terms to the master equation to counteract the runaway energy increase,
- non Markovian correlation function.

In both cases characteristic energy dependence of the spontaneous emission rate is expected!<sup>21</sup>

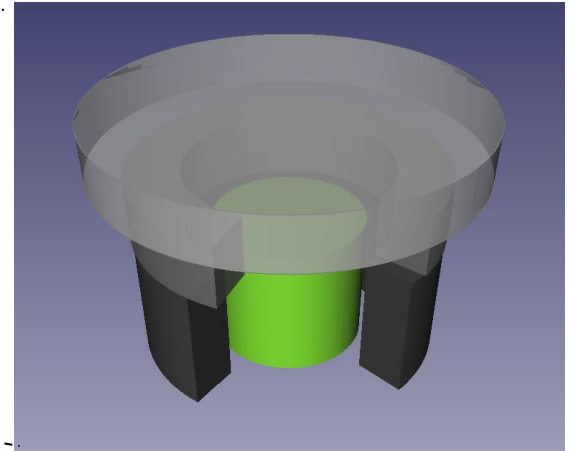
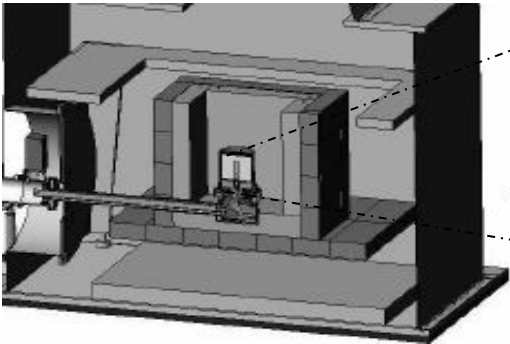
*Continuous Spontaneous Localization model ..*

*constraint on the  $\Lambda/r_c^2$  parameters*

# Pb target HPGe detector

- Ge detector surrounded by Roman lead target + complex electrolytic Cu + Pb shielding
- $^{10}\text{B}$ -polyethylene plates reduce the neutron flux towards the detector
- shield + cryostat enclosed in air tight steel housing flushed with nitrogen to avoid contact with external air (and thus radon).

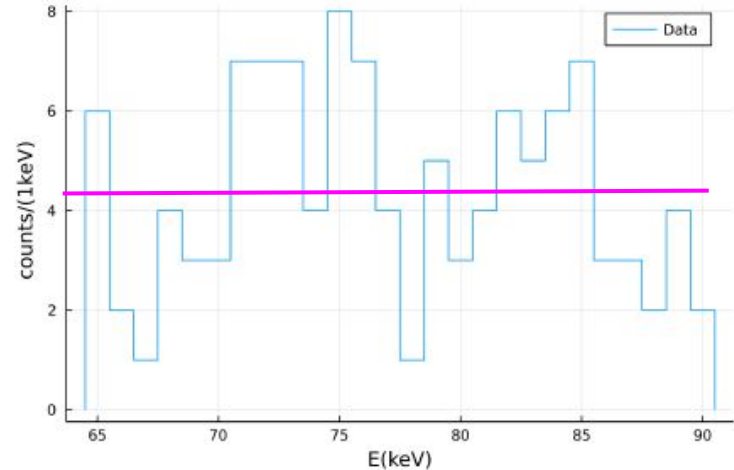
*K. Piscicchia et al., Eur. Phys. J. C (2020) 80: 508*



# Pb target HPGe detector

- Factor two gain in background reduction,
- available sensitive energy range extended (30 - 3800) keV
- Considering the energy resolution (better than 0.5 keV in this range), from a study of the materials of the apparatus the only eventual detectable transitions in  $\Delta E = (65-90)$  keV would correspond to the K complex in Pb.

Result of a maximum likelihood fit to the bkg spectrum



# CSL in few words

The dynamics is characterized by the interaction with a continuous set of independent noises (one for each point of the space) having, under the simplest assumption, zero average and white correlation in time.

The new stochastic terms require the introduction of two phenomenological quantities:

- a collapse rate  $\lambda$ , which sets the strength of the collapse
- a noise correlation length  $r_c$  which measures the spatial resolution of the collapse

Various theoretical considerations lead to different choices for the parameters:

- Ghirardi, Rimini and Weber:  $\lambda = 10^{-17} \text{ s}^{-1}$  and  $r_c = 10^7 \text{ m}$ ,
- Adler:  $\lambda = 10^{-8} \text{ s}^{-1}$  for  $r_c = 10^7 \text{ m}$ , and  $\lambda = 10^{-6} \text{ s}^{-1}$  for  $r_c = 10^6 \text{ m}$ .

# Expected rate of spontaneous radiation

*The new stochastic terms require the introduction of two phenomenological quantities:*

- *a collapse rate  $\lambda$ , which sets the strength of the collapse*
- *a noise correlation length  $r_c$  which measures the spatial resolution of the collapse*

$$\left. \frac{d\Gamma}{dE} \right|_t = N_{atoms} \cdot (N_A^2 + N_A) \cdot \frac{\hbar e^2}{4 \pi^2 \epsilon_0 c^3 m_0^2} \cdot \frac{\lambda}{r_C^2} \frac{1}{E}$$

# Philosophy of the analysis

Aim is to get the pdf of  $\lambda/r_C^2$   $P(\lambda/r_C^2|data) = \int_{\mathcal{D}_b} P(\lambda/r_C^2, \mathbf{b}|data) d\mathbf{b}$ ,

$\mathbf{b}$  is the vector of parameters characterizing the bkg shape.

$$P(\lambda/r_C^2, \mathbf{b}|data) = \frac{P(data|\lambda/r_C^2, \mathbf{b}) \cdot P_0(\lambda/r_C^2) \cdot P_0(\mathbf{b})}{\int P(data|\lambda/r_C^2, \mathbf{b}) \cdot P_0(\lambda/r_C^2) \cdot P_0(\mathbf{b}) d\left(\frac{\lambda}{r_C^2}\right) d\mathbf{b}},$$

Likelihood:

$$P(data|\lambda/r_C^2, \mathbf{b}) = \prod_{i=1}^N \frac{\lambda_i(\lambda/r_C^2, \mathbf{b})^{n_i} \cdot e^{-\lambda_i(\lambda/r_C^2, \mathbf{b})}}{n_i!}$$

$$\lambda_i(\lambda/r_C^2, \mathbf{b}) = \int_{\Delta E_i} f_B(E, \mathbf{b}) dE + \int_{\Delta E_i} f_S(E, \lambda/r_C^2) dE.$$

# Philosophy of the analysis

Aim is to get the pdf of  $\lambda/r_C^2$   $P(\lambda/r_C^2|data) = \int_{\mathcal{D}_b} P(\lambda/r_C^2, \mathbf{b}|data) d\mathbf{b}$ ,

$\mathbf{b}$  is the vector of parameters characterizing the bkg shape.

$$P(\lambda/r_C^2, \mathbf{b}|data) = \frac{P(data|\lambda/r_C^2, \mathbf{b}) \cdot P_0(\lambda/r_C^2) \cdot P_0(\mathbf{b})}{\int P(data|\lambda/r_C^2, \mathbf{b}) \cdot P_0(\lambda/r_C^2) \cdot P_0(\mathbf{b}) d\left(\frac{\lambda}{r_C^2}\right) d\mathbf{b}}$$

Likelihood:

$$P(data|\lambda/r_C^2, \mathbf{b}) = \prod_{i=1}^N \frac{\lambda_i(\lambda/r_C^2, \mathbf{b})^{n_i} \cdot e^{-\lambda_i(\lambda/r_C^2, \mathbf{b})}}{n_i!}$$

$$\lambda_i(\lambda/r_C^2, \mathbf{b}) = \int_{\Delta E_i} f_B(E, \mathbf{b}) dE + \int_{\Delta E_i} f_S(E, \lambda/r_C^2) dE.$$

Bkg and signal shapes

# Expected signal shape

$$f_S(E, \lambda/r_C^2) = T \beta \frac{\lambda}{r_C^2} E^{-1} \sum_j \alpha_j \epsilon_j(E) = T \beta \frac{\lambda}{r_C^2} E^{-1} \sum_j \alpha_j \sum_{k=0}^{d_j} \xi_{jk} E^k$$

$$\beta = \frac{\hbar e^2}{4 \pi^2 \epsilon_0 c^3 m_0^2}$$

$$\alpha_j = m_j n_j \cdot (N_{pj}^2 + N_{ej}^2)$$

Table 1. The table summarises the parameters obtained from the best fit to the efficiency spectra, for each component of the setup which gives a significant contribution.

$j =$	Ge crystal	Pb target
$\xi_{j0}$	$(9.68 \pm 0.12) \cdot 10^{-1}$	$(-1.40 \pm 5.6) \cdot 10^{-4}$
$\xi_{j1}$	$(1.72 \pm 0.41) \cdot 10^{-3}$	$(0.08 \pm 1.18) \cdot 10^{-5}$
$\xi_{j2}$	$(-2.14 \pm 0.56) \cdot 10^{-5}$	$(2.84 \pm 5.57) \cdot 10^{-8}$
$\xi_{j2}$	$(-1.37 \pm 0.65) \cdot 10^{-7}$	-
$\xi_{j2}$	$(1.32 \pm 0.49) \cdot 10^{-9}$	-

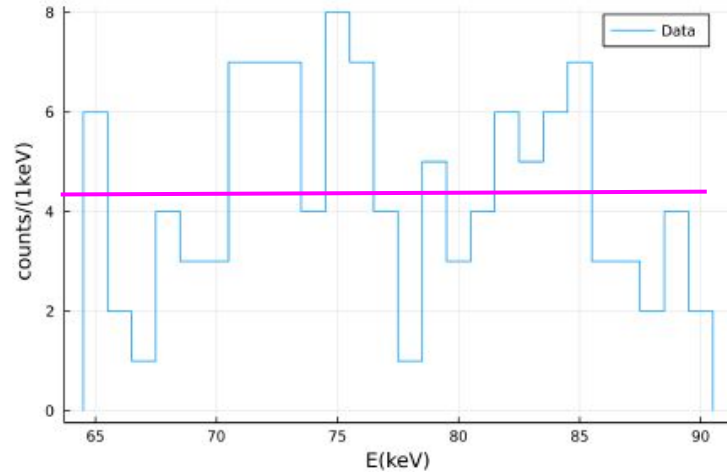
- *The resolution of the detector is constant (equal to  $0.49 \pm 0.04$  keV) over  $\Delta E \rightarrow$  smearing correction to the theoretical expected shape is not needed.*
- *$\lambda/r_C^2$  uniform prior between 0 and 52*

# Background shape

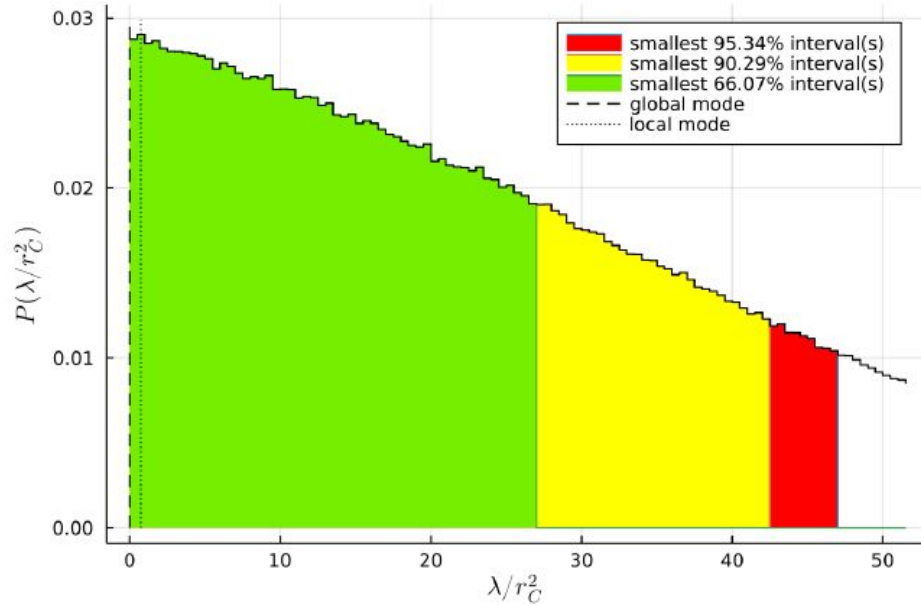
$$f_B(E, \mathbf{b}) = b_1 + E \cdot b_2$$

*We leave free the parameters characterizing the bkg shape.*

$$b_1 \in [0, 20] \quad ; \quad b_2 \in [-1, 1].$$



# Posterior & cumulative distributions



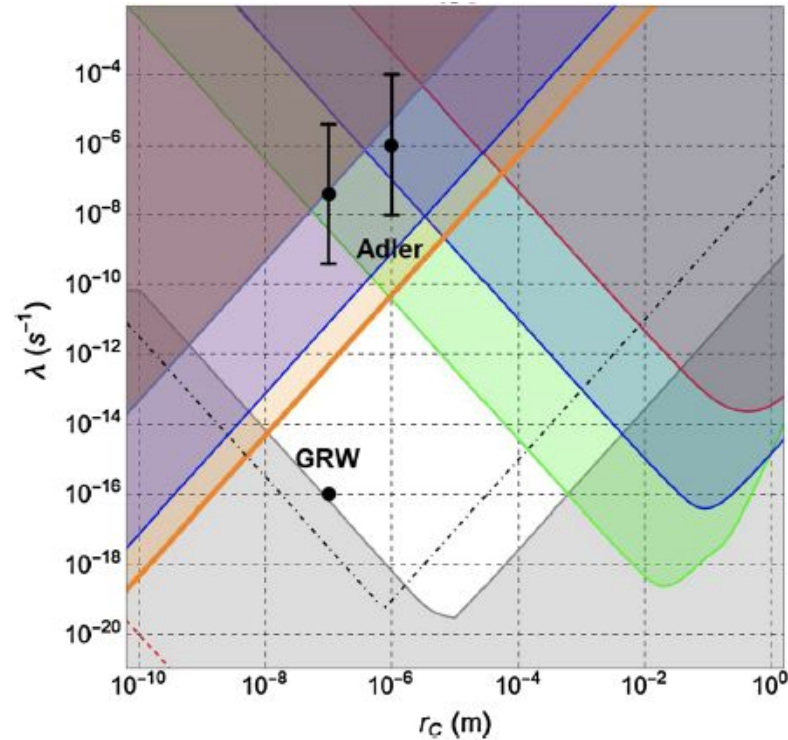
$$\tilde{P}(\mathcal{L}) = \int_0^{\mathcal{L}} P(\lambda/r_C^2 | data) d\left(\frac{\lambda}{r_C^2}\right) = \Pi.$$

$$\frac{\lambda}{r_C^2} < 47 \text{ s}^{-1} \text{ m}^{-2}$$

with probability 0.95

# Posterior & cumulative distributions

Which yields  $\lambda < 4.7 \cdot 10^{-13} \text{ s}^{-1}$  for  $r_c = 10^{-7} \text{ m}$  with probability 0.95



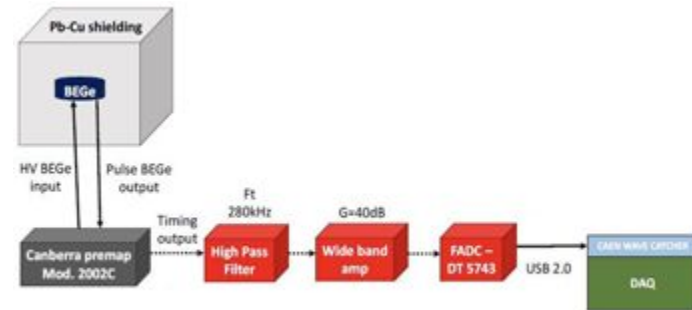
*Ongoing experimental activity  
and development of new detector systems*

# Development of a new detector system - BE - HPGe

*Most sensitive experimental survey of spontaneous radiation emission to test dissipative & non-Markovian Collapse Models. Strategy:*

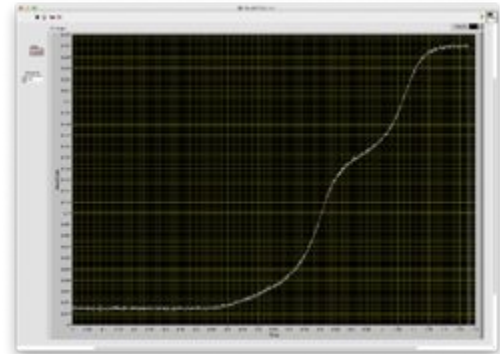
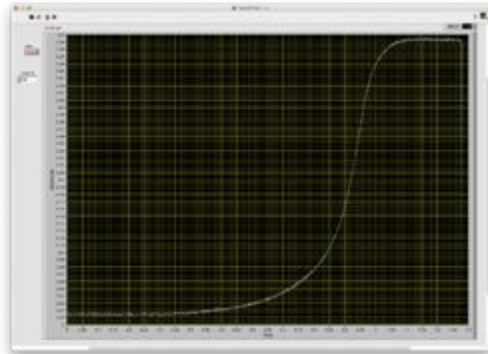
- *BE-HPGe, combined to an innovative readout electronics, will be employed as an active detector,*
- *extreme radio-purity Roman lead target will serve as an active shielding*

*electric field configuration of the BE-HPGe detector + flash ADC + dedicated readout electronics + pulse shape analysis -> to push down to few KeV the lower energy detection limit -> increase of the expected spontaneous radiation signal.*



# Development of a new detector system - BE - HPGe

Single site event (left) and multiple site events (right) generated within the BE-HPGe acquired by the Front-End electronics



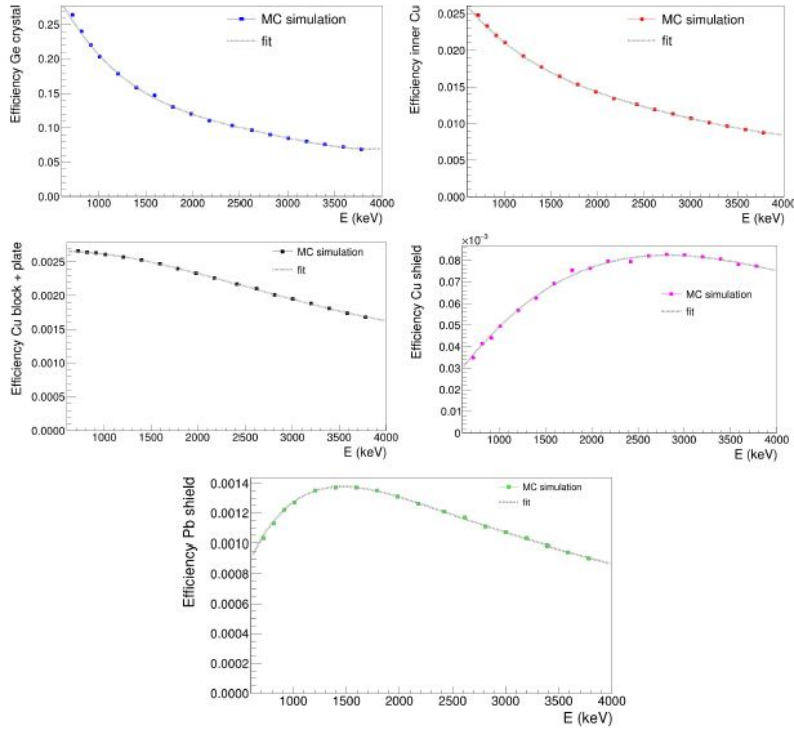
Connection of the Front-End electronic to the BEGe's Canberra preamplifier (Mod. 2002C), behind the liquid N<sub>2</sub> dewar

*Thank you*

# Bounds on $\lambda$ and $r_C$ parameters of the CSL model

## expected signal contribution

The expected signal of spontaneously emitted photons by the nuclei of all the materials of the detector is obtained weighting the theoretical rate for the detection efficiencies:



- $10^8$  photons generated for each energy for each material
- efficiency functions are obtained by polynomial fits  $\epsilon_i(E) = \sum_{j=0}^{c_i} \xi_{ij} E^j$
- the expected signal contribution is:

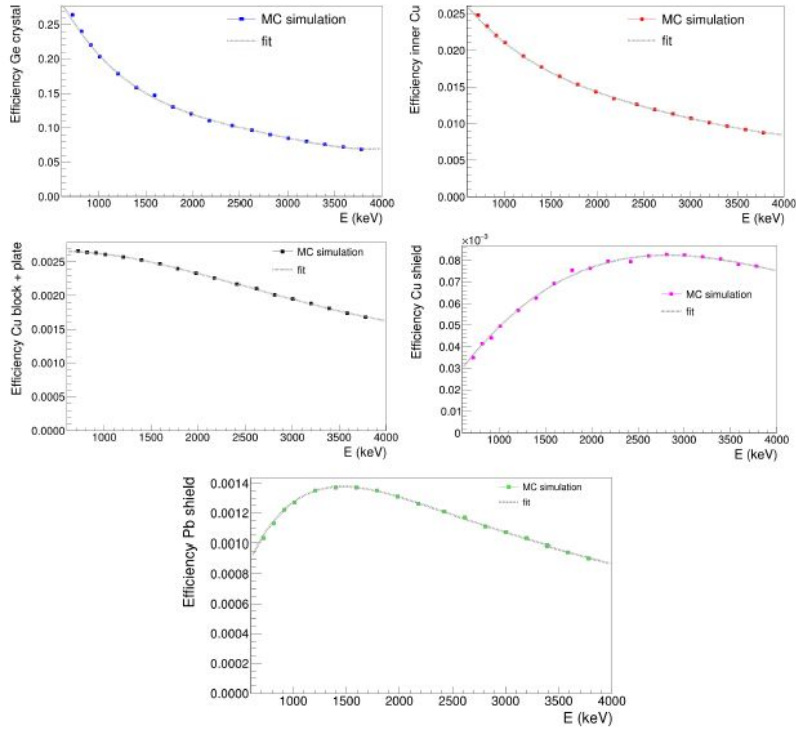
$$z_s \left( \frac{\lambda}{r_C^2} \right) = \sum_i \int_{\Delta E} \frac{d\Gamma}{dE} \Big|_i \epsilon_i(E) dE =$$

$$= 1.83828 \frac{\lambda}{r_C^2} = a \frac{\lambda}{r_C^2}$$

# Bounds on $\lambda$ and $r_C$ parameters of the CSL model

## expected signal contribution

The expected number of photons spontaneously emitted by the nuclei of all the materials of the detector are obtained weighting the theoretical rate for the detection efficiencies:



- $10^8$  photons generated for each energy for each material
- efficiency functions are obtained by polynomial fits  $\epsilon_i(E) = \sum_{j=0}^{c_i} \xi_{ij} E^j$
- the expected signal contribution is:

$$z_s \left( \frac{\lambda}{r_C^2} \right) = \sum_i \int_{\Delta E} \frac{d\Gamma}{dE} \Big|_i \epsilon_i(E) dE = 1.83828 \frac{\lambda}{r_C^2} = a \frac{\lambda}{r_C^2}$$

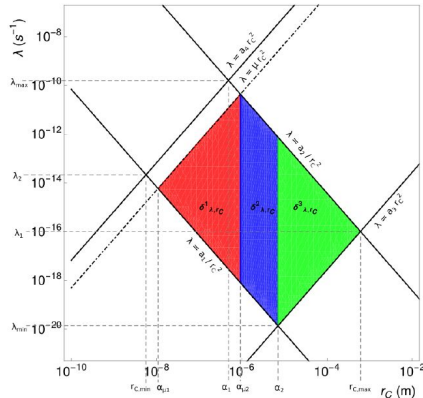
# Bounds on $\Lambda$ and $r_c$ parameters of the CSL model

## joint pdf of $\Lambda$ and $r_c$ stochastic variables

$z_c$  is distributed according to a Poissonian  $p(z_c|\Lambda_c) = \frac{\Lambda_c^{z_c} e^{-\Lambda_c}}{z_c!}$  with  $\Lambda_c \left( \frac{\lambda}{r_c^2} \right) = \Lambda_b + \Lambda_s \left( \frac{\lambda}{r_c^2} \right)$

in terms of the parameters  $\Lambda$  and  $r_c$  this is a generic pdf  $p(z_c|\lambda, r_c) = \frac{\left( a \frac{\lambda}{r_c^2} + \Lambda_b + 1 \right)^{z_c} e^{-\left( a \frac{\lambda}{r_c^2} + \Lambda_b + 1 \right)}}{z_c!}$

by probability inversion:  $\tilde{p}(\lambda, r_c) = \frac{\left( a \frac{\lambda}{r_c^2} + \Lambda_b + 1 \right)^{z_c} e^{-\left( a \frac{\lambda}{r_c^2} + \Lambda_b + 1 \right)} \cdot \tilde{p}_0(\lambda, r_c)}{\int_{D_{\lambda, r_c}} \left( a \frac{\lambda}{r_c^2} + \Lambda_b + 1 \right)^{z_c} e^{-\left( a \frac{\lambda}{r_c^2} + \Lambda_b + 1 \right)} dr_c d\lambda}$



the prior reduces the domain  $\mathbb{R}^{2+}$  to the region allowed by experiments and theory

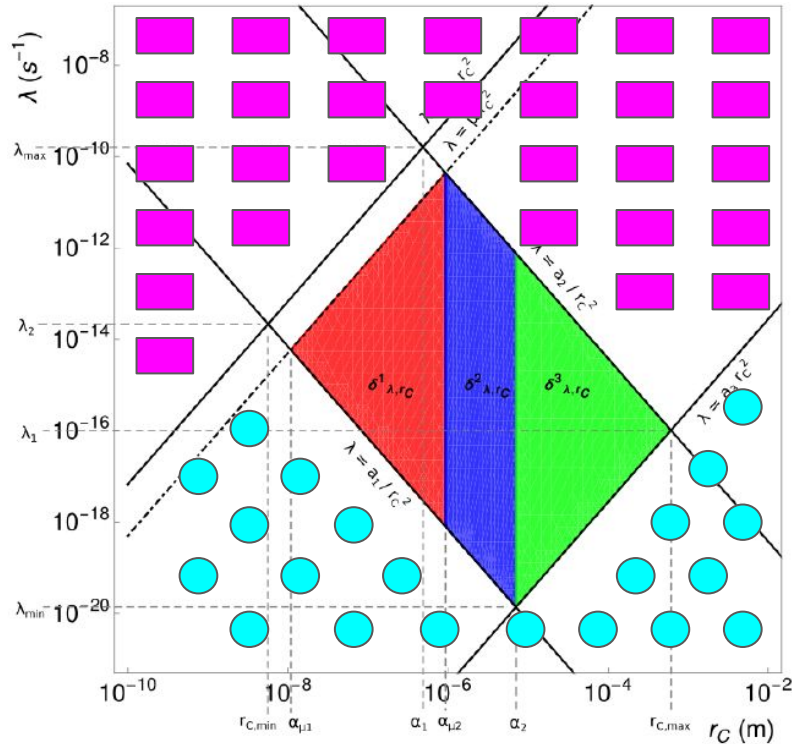
$$\tilde{p}_0(\lambda, r_c) = \vartheta\left(\lambda - \frac{a_1}{r_c^2}\right) \cdot \vartheta\left(\frac{a_2}{r_c^2} - \lambda\right) \cdot \vartheta(\lambda - a_3 r_c^2) \cdot \vartheta(a_4 r_c^2 - \lambda)$$

# Bounds on $\Lambda$ and $r_c$ parameters of the CSL model

joint pdf of  $\Lambda$  and  $r_c$  stochastic variables

the prior reduces the domain  $\mathbb{R}^{2+}$  to the region allowed by experiments and theory,

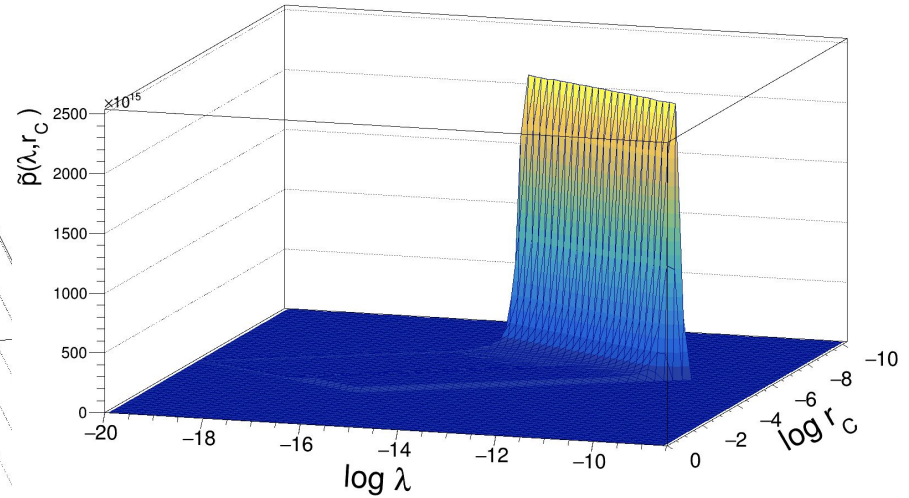
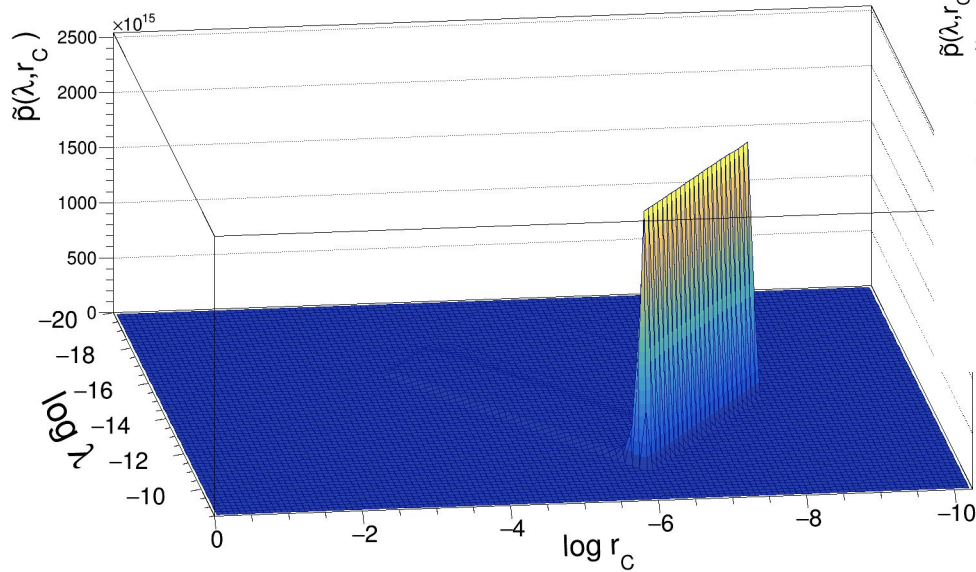
see Ref. [M. Carlesso and S. Donadi, *Advances in Open Systems and Fundamental Tests of Quantum Mechanics*, Ed. B. Vacchini and H.-P. Breuer and A. Bassi (2019), p. 1-13], and A. Bassi's, H. Ulbricht's, P. Barker's talks



- excluded by the theory
- excluded by experiments

# Bounds on $\Lambda$ and $r_c$ parameters of the CSL model

joint pdf of  $\Lambda$  and  $r_c$  stochastic variables



# Bounds on $\Lambda$ and $r_c$ parameters of the CSL model

excluding domains bordered by  $\Lambda = \mu \cdot r_c^2$

Given that the expected rate of spontaneous radiation is proportional to  $\Lambda / r_c^2$  it makes sense to investigate:

- upper limits on  $\Lambda$
  - lower limits on  $r_c$
  - constraining the expected number of spontaneously emitted photons i.e.  $\Lambda / r_c^2$ .
- for which we need the corresponding pdfs

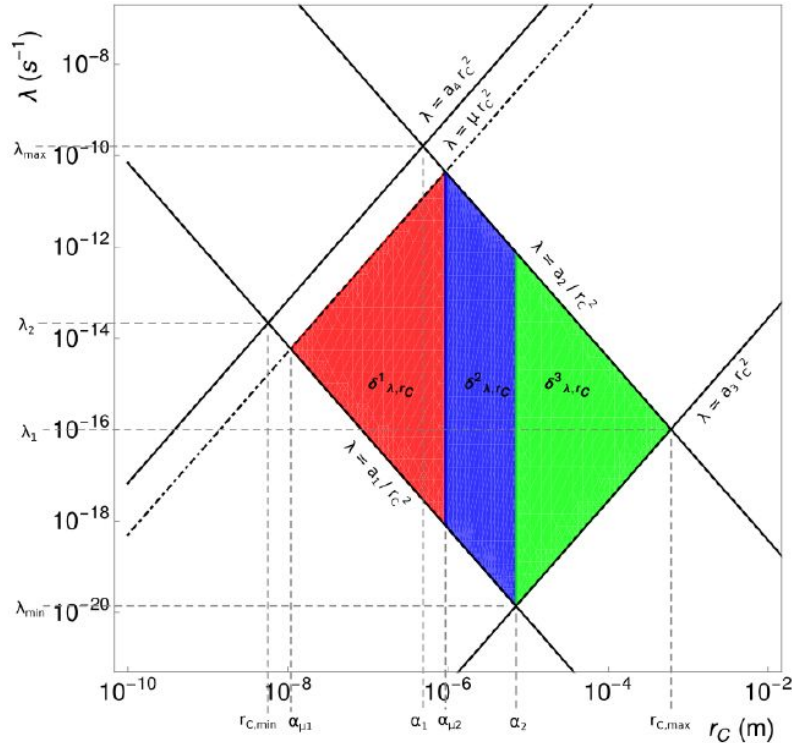
In the latter case we have to solve the equation:

$$\tilde{P}(\mu) = \frac{1}{\mathcal{N}} \left[ \iint_{\delta_{\lambda, r_c}^1} p(z_c | \lambda, r_c) d\lambda dr_c + \iint_{\delta_{\lambda, r_c}^2} p(z_c | \lambda, r_c) d\lambda dr_c + \iint_{\delta_{\lambda, r_c}^3} p(z_c | \lambda, r_c) d\lambda dr_c \right] = \Pi$$

with  $\mathcal{N}$  being the normalisation and  $\Pi$  the desired probability level.

# Bounds on $\Lambda$ and $r_c$ parameters of the CSL model excluding domains bordered by $\Lambda = \mu \cdot r_c^2$

The three integration domains correspond to the **red**, **blue** and **green** regions below:



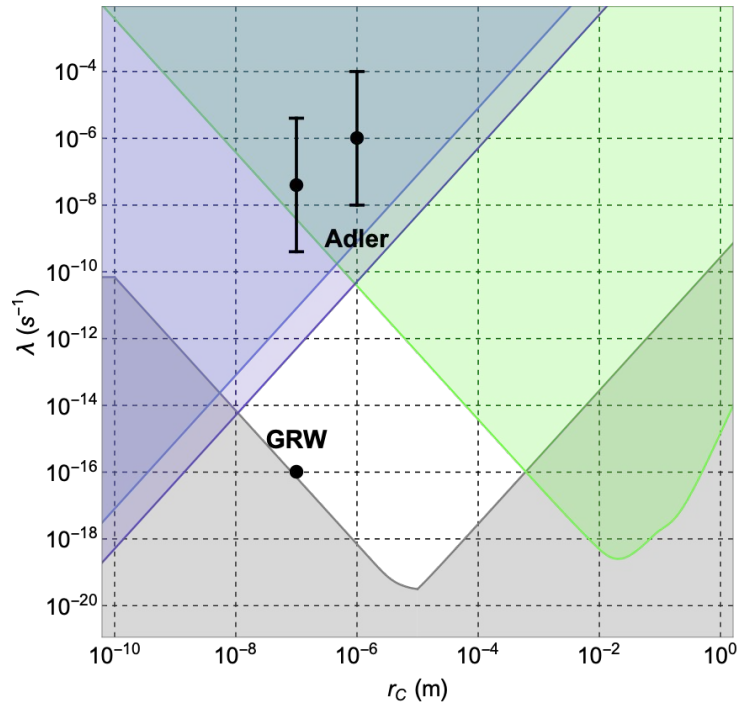
they vary with the parameter  $\mu$  and the corresponding bound is shown as a dash-dot line

-----

# Bounds on $\Lambda$ and $r_c$ parameters of the CSL model

excluding domains bordered by  $\Lambda = \mu \cdot r_c^2$

By solving the equation for a probability  $\Pi = 0.9$  we obtain  $\Lambda < 50.7 \cdot r_c^2$  which improves our previous result of a factor 13 ...



this work upper bound on  $\Lambda/r_c^2$



K. Piscicchia et al., *Entropy* 2017,  
19(7), 319

C. Curceanu, K. Piscicchia et al,  
*International Journal of Quantum  
Information* Vol. 17, No. 8 (2019)  
1941011

preliminary

# Bounds on $\Lambda$ and $r_c$ parameters of the CSL model

## pdf of $\Lambda$

In order to obtain the pdf of the parameter  $\Lambda$  we have to marginalize the joint pdf with respect to  $r_c$ . Due to the priors the functional dependence  $r_c(\Lambda)$  changes in different intervals of the domain of  $\Lambda$ , hence the pdf is piecewise-defined:

$$\tilde{p}(\lambda) = \begin{cases} \tilde{p}_1(\lambda) = \frac{1}{\mathcal{N}} \int_{\sqrt{a_1/\lambda}}^{\sqrt{\lambda/a_3}} \left( a \frac{\lambda}{r_c^2} + \Lambda_b + 1 \right)^{z_c} e^{-\left( a \frac{\lambda}{r_c^2} + \Lambda_b + 1 \right)} dr_c & \lambda_{min} \geq \lambda > \lambda_1 \\ \tilde{p}_2(\lambda) = \frac{1}{\mathcal{N}} \int_{\sqrt{a_1/\lambda}}^{\sqrt{a_2/\lambda}} \left( a \frac{\lambda}{r_c^2} + \Lambda_b + 1 \right)^{z_c} e^{-\left( a \frac{\lambda}{r_c^2} + \Lambda_b + 1 \right)} dr_c & \lambda_1 \geq \lambda > \lambda_2 \\ \tilde{p}_3(\lambda) = \frac{1}{\mathcal{N}} \int_{\sqrt{\lambda/a_4}}^{\sqrt{a_2/\lambda}} \left( a \frac{\lambda}{r_c^2} + \Lambda_b + 1 \right)^{z_c} e^{-\left( a \frac{\lambda}{r_c^2} + \Lambda_b + 1 \right)} dr_c & \lambda_2 \geq \lambda > \lambda_{max} \end{cases}$$

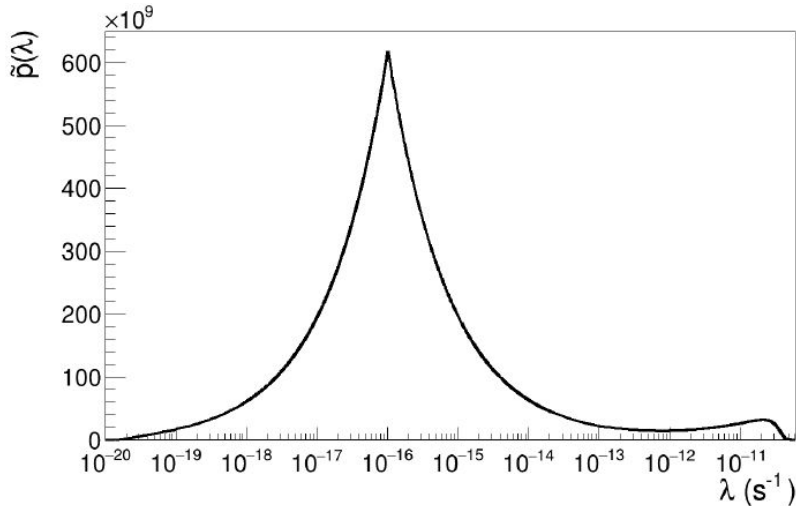
# Bounds on $\Lambda$ and $r_c$ parameters of the CSL model

## pdf of $\Lambda$

The integrals admit analytical solution, which yields the following shape:

$$M_i(\lambda) = \sum_{k=0}^{z_c} \binom{z_c}{k} \left( -\frac{(a\lambda)^{1/2}}{2} \right) e^{-(\Lambda_b+1)} (\Lambda_b + 1)^{z_c-k} \int_{\frac{a\lambda}{l_1^2}}^{\frac{a\lambda}{l_2^2}} \xi^{k-\frac{3}{2}} e^{-\xi} d\xi =$$

$$= \sum_{k=0}^{z_c} \binom{z_c}{k} \left( -\frac{(a\lambda)^{1/2}}{2} \right) e^{-(\Lambda_b+1)} (\Lambda_b + 1)^{z_c-k} \cdot \left[ \gamma \left( k - \frac{1}{2}, \frac{a\lambda}{l_2^2} \right) - \gamma \left( k - \frac{1}{2}, \frac{a\lambda}{l_1^2} \right) \right]$$



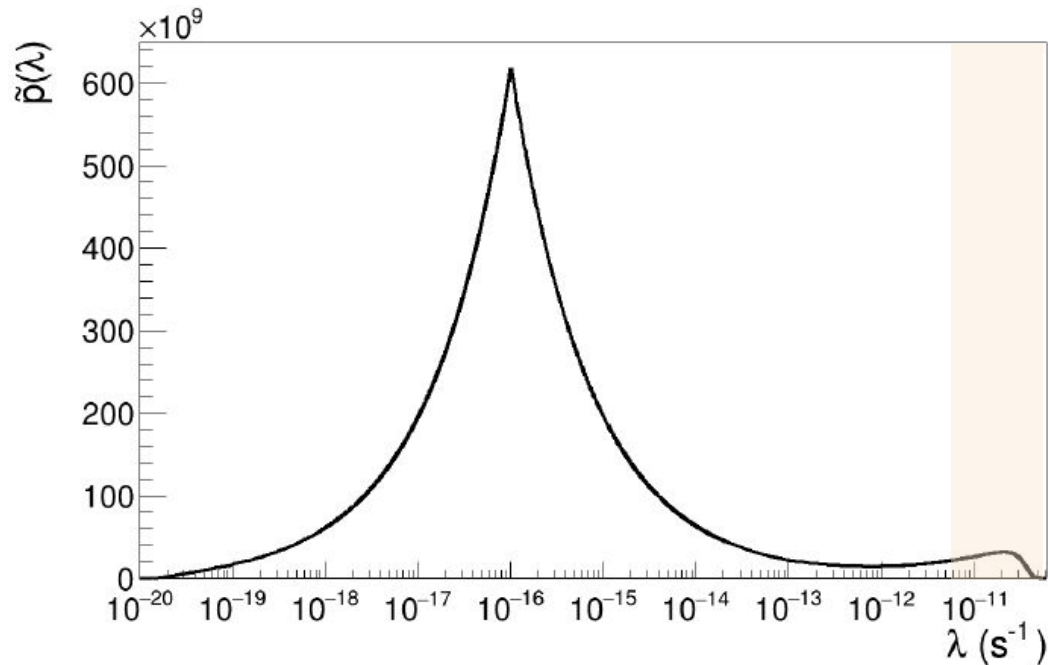
And, for the three intervals, the cumulative pdf:

$$\tilde{P}(\bar{\lambda}) = \begin{cases} \int_{\lambda_{\min}}^{\bar{\lambda}} \tilde{p}_1(\lambda) d\lambda \\ \int_{\lambda_{\min}}^{\lambda_1} \tilde{p}_1(\lambda) d\lambda + \int_{\lambda_1}^{\bar{\lambda}} \tilde{p}_2(\lambda) d\lambda \\ \int_{\lambda_{\min}}^{\lambda_1} \tilde{p}_1(\lambda) d\lambda + \int_{\lambda_1}^{\lambda_2} \tilde{p}_2(\lambda) d\lambda + \int_{\lambda_2}^{\bar{\lambda}} \tilde{p}_3(\lambda) d\lambda \end{cases}$$

# Bounds on $\Lambda$ and $r_c$ parameters of the CSL model

## pdf of $\Lambda$

By equating the cumulative pdf to a probability  $\Pi = 0.9$  we obtain  $\Lambda < \bar{\Lambda} = 3.5 \cdot 10^{-11} \text{ s}^{-1}$



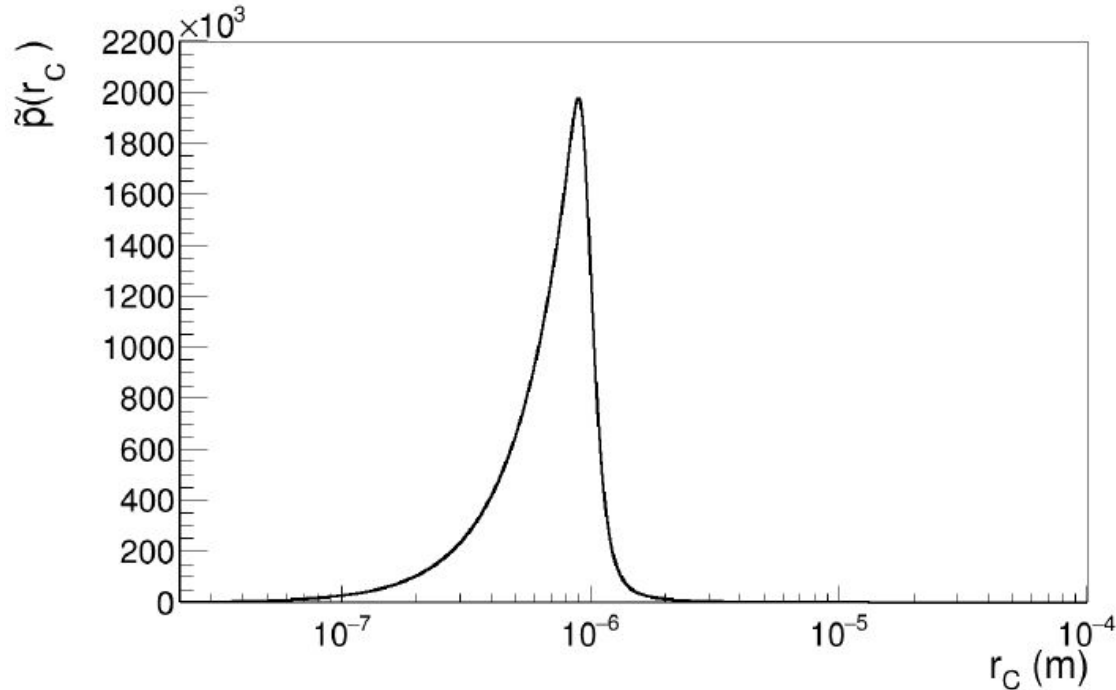
upper bound on  $\Lambda$

preliminary

# Bounds on $\Lambda$ and $r_c$ parameters of the CSL model

## pdf of $r_c$

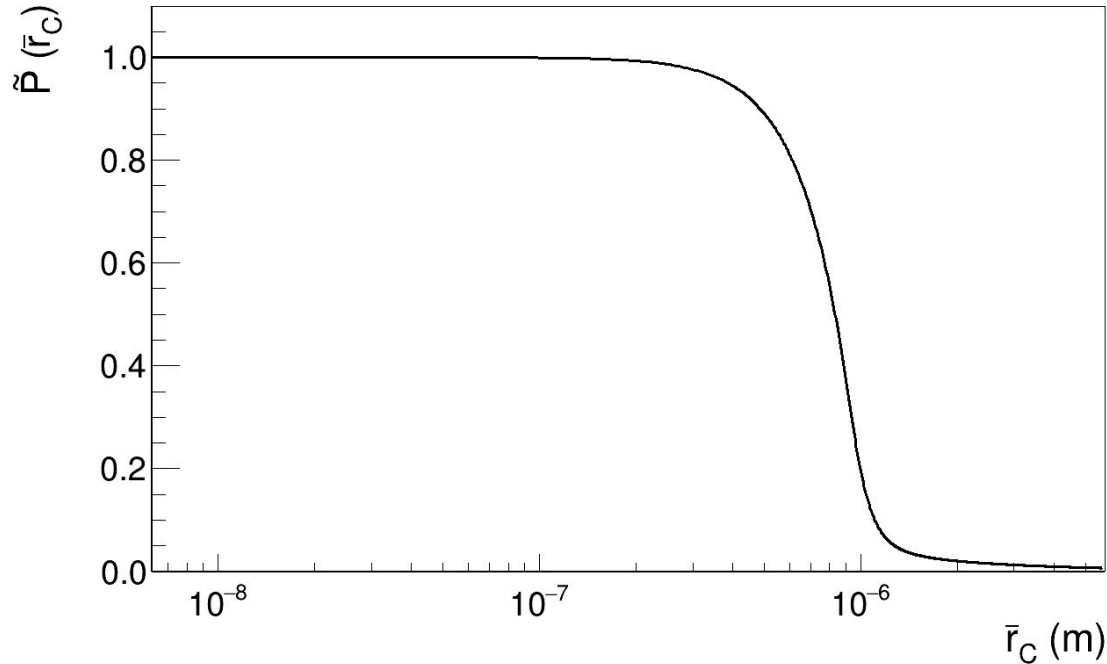
In complete analogy, to obtain the pdf of  $r_c$  we have to marginalise with respect to  $\Lambda$  which yields:



# Bounds on $\Lambda$ and $r_c$ parameters of the CSL model

pdf of  $r_c$

*This time we are interested to the complementary cumulative pdf:*

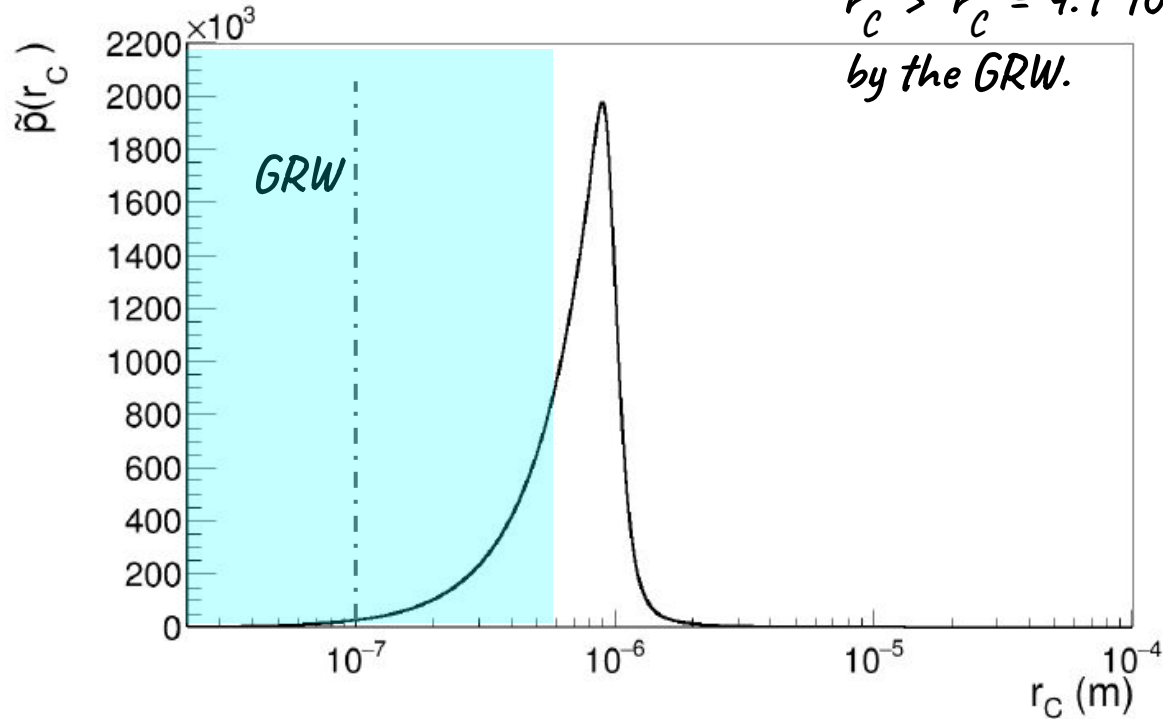


# Bounds on $\Lambda$ and $r_c$ parameters of the CSL model

pdf of  $r_c$

By equating the complementary cumulative pdf to a probability  $\Pi = 0.9$  we obtain:

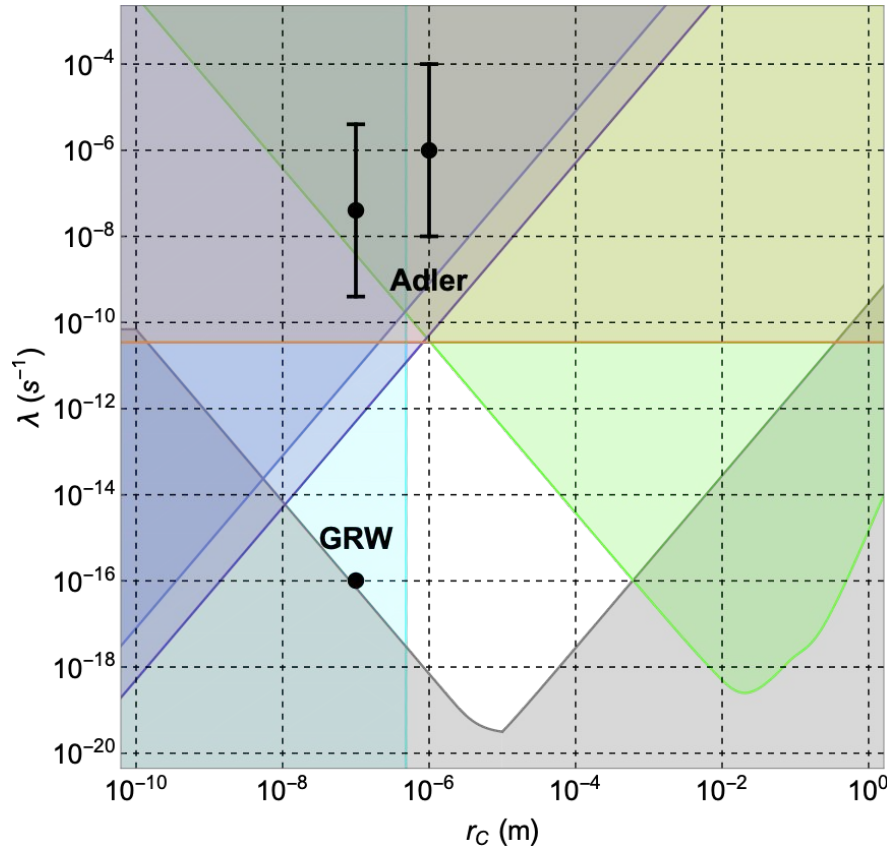
$r_c > \bar{r}_c = 4.9 \cdot 10^{-7} \text{ m}$  which exceeds the value proposed by the GRW.



upper bound on  $r_c$

preliminary

# Bounds on $\Lambda$ and $r_c$ parameters of the CSL model



*Stronger existent constraint in  
the parameters space*

*To be submitted to PRL*

*preliminary*